**Cluster Basicity.** In strongly acidic media Davidson et al.[40] discovered that metal carbonyl compounds can undergo protonation. Later, infrared and $^1H$ NMR data were reported for $HOs_3(CO)_{12}^+$, $HRu_3(CO)_{12}^+$, $H_2Ir_4(CO)_{12}^{2+}$, and a variety of $H_2Os_3(CO)_{12-x}(L)_x^{2+}$ complexes.[41,42] All of these compounds were prepared by dissolution in 98% $H_2SO_4$. Knight and Mays[42] reported infrared data for $Ru_3(CO)_{12}$ and $Os_3(CO)_{12}$ in neat trifluoroacetic acid. Although they did not assign them as such it is apparent that the species present are the protonated clusters. Subsequent solution NMR studies[41] and inelastic neutron-scattering experiments[43] supported edge protonation in $[HRu_3(CO)_{12}]^+$ and $[HOs_3(CO)_{12}]^+$. The miscibility of trifluoroacetic acid with organic solvents allowed us to titrate (Supplementary Figure 1) the trinuclear clusters to the monoprotonated species in $CH_2Cl_2$ solution. The protonated osmium complex exhibits absorptions with $\lambda_{max}$ ($\epsilon$) 369 (8800), 305 (6400), and 275 nm (sh). Bands at $\lambda_{max}$ ($\epsilon$) 400 (1100), 345 (sh), 286 (sh), and 270 nm (8100) characterize the ruthenium analogue. Protonation blue shifts the spectra and leaves one low-energy transition. Recall that the plot for the $10a_1' \rightarrow 6a_2'$ transition showed little change in the electron density along the edge of the $Ru_3$ cluster. Provided that orbital hybridization does not change greatly, this transition's energy would only slightly vary upon edge protonation. Lowering the symmetry now provides electric dipole intensity. From spectrophotometric titrations,[44] the osmium cluster appears to be 5 times more basic than the ruthenium analogue. A similarity in the proton-acceptor ability of $Ru_3(CO)_{12}$ and $Os_3(CO)_{12}$ conforms with their similar first IP's, net d-electron populations, and orbital splittings.

**Acknowledgment.** We thank the National Resource for Computation in Chemistry for a grant of computer time. This work was supported in part by the National Science Foundation, Grant DMR79-25379. Work performed at ANL was done under the auspices of the Division of Basic Energy Sciences of the U.S. Department of Energy. Professor Duward Shriver generously provided us access to his Raman spectrometer.

**Registry No.** $Ru_3(CO)_{12}$, 15243-33-1; $Os_3(CO)_{12}$, 15696-40-9.

**Supplementary Material Available:** Tables of orbital energies for the SCC-DV-X$\alpha$ calculations of $Os_3(CO)_{12}$ and $Ru_3(CO)_{12}$ and the MP-DV-X$\alpha$ calculation of $Os_3(CO)_{12}$, IP's from all four calculations, and atomic populations from the four calculations and a figure of the titration of $Os_3(CO)_{12}$ with $HO_2CCF_3$ in $CH_2Cl_2$ (4 pages). Ordering information is given on any current masthead page.

(40) Davidson, A.; McFarlane, W.; Pratt, L.; Wilkinson, G. *J. Chem. Soc.* **1962**, 3653.
(41) Deeming, A. J.; Johnson, B. F. G.; Lewis, J. *J. Chem. Soc. A* **1970**, 2967-2971. Koridze, A. A.; Kizas, O. A.; Astakhova, N. M.; Petrovskii, P. V.; Grishin, Y. K. *J. Chem. Soc., Chem. Commun.* **1981**, 853-855.
(42) Knight, J.; Mays, M. J. *J. Chem. Soc. A* **1970**, 711-714.
(43) White, J. W.; Wright, W. *J. Chem. Soc. A* **1971**, 2843-2847.
(44) Hammett, L. P. "Physical Organic Chemistry"; McGraw-Hill: New York, 1970.

Contribution from the Institut für Anorganische, Analytische und Physikalische Chemie der Universität Bern, CH-3000 Bern 9, Switzerland

# Low-Temperature Structural and Spectroscopic Properties of $[Cr_3O(CH_3COO)_6(H_2O)_3]Cl \cdot 6H_2O$

KURT J. SCHENK and HANS U. GÜDEL*

*Received November 3, 1981*

The structural properties of the title compound were studied by X-ray diffraction at 190 K. The compound undergoes a structural phase transition at 211 K. HT and LT space groups are $P2_12_12$ and $P2_12_12_1$, respectively. The LT unit cell is twice as long in the *c* direction as the HT cell, with *a* and *b* unchanged. In the LT structure, there are two inequivalent sets a and b of triangular clusters. Measurements of the luminescence spectra, decay curves, and time-resolved spectra in the temperature range 7-83 K revealed that there is no excitation energy transfer (ET) between clusters at 7 K. With increasing temperature, ET sets in; and an upper limit estimate for the transfer rate from set a to b clusters at 83 K is $9 \times 10^4$ s$^{-1}$. A value of 0.1 cm$^{-1}$ is obtained as an upper limit estimate for the intercluster exchange parameter. The LT magnetic and spectroscopic properties result from geometrical distortions of triangular clusters.

## 1. Introduction

The chloride salt of basic chromium(III) acetate (abbreviated CRAC in the following) has been the subject of a large number of experimental and theoretical studies. The principal aim of the majority of those investigations was an understanding of the exchange effects responsible for the unusual low-temperature (LT) thermal and magnetic properties. In a recent article by Brown and co-workers, the earlier work in this area was briefly reviewed.[1]

At room temperature the chromium(III) ions of the trimeric complexes form equilateral triangles within the rather low accuracy of the crystal structure determination.[2] The clusters are well separated and insulated from one another by the bulky ligands and the highly disordered water/anion structure. The shortest intercluster Cr-Cr distance is 5.78 Å, as compared to 3.27 Å within the trimers. At 211 K CRAC undergoes a first-order structural phase transition.[3] Whereas all the trimeric complexes are crystallographically equivalent in the high-temperature (HT) phase, there are two sets of inequivalent complexes in the LT phase.[4]

A very detailed and accurate description of exchange splittings in both sets a and b of clusters was obtained from absorption and luminescence spectra.[4] On the basis of a model originally proposed by Sorai and co-workers[3] to rationalize the LT heat capacity of CRAC, the observed electronic splittings were interpreted as resulting from geometrically distorted triangular complexes.[4] Since there was no direct experimental evidence for the existence of distorted complexes in the LT

(1) Wrobleski, J. T.; Dziobkowski, C. T.; Brown, D. B. *Inorg. Chem.* **1981**, *20*, 684.
(2) Chang, S. C.; Jeffrey, G. A. *Acta Crystallogr., Sect. B* **1970**, *B26*, 673.
(3) Sorai, M.; Tachiki, M.; Suga, H.; Seki, S. *J. Phys. Soc. Jpn.* **1971**, *30*, 750.
(4) Ferguson, J.; Güdel, H. U. *Chem. Phys. Lett.* **1972**, *17*, 547.

0020-1669/82/1321-2253$01.25/0 

Table I. Unit Cell Dimensions (Å) and Space Groups of the HT and LT Phases of CRAC

| $T$ = 190 K, LT phase | | $T$ = 298 K, HT phase | |
|---|---|---|---|
| $P2_12_12_1$ | $a$ = 13.582 (4) Å | $P2_12_12$ | $a$ = 13.677 (10) Å |
| $Z$ = 8 | $b$ = 23.177 (7) Å | $Z$ = 4 | $b$ = 23.141 (18) Å |
| | $c$ = 18.156 (4) Å | | $c$ = 9.142 (7) Å |

phase, this interpretation was recently challenged by Brown and co-workers.[1] In these authors' opinion, intercluster exchange interactions rather than intracluster geometrical distortions were responsible for the observed effects.[1] Intercluster exchange parameters of 2.4 and 0.6 $cm^{-1}$ were proposed. This is an interesting proposition because very little is known about the interplay of intra- and intermolecular interactions in compounds of this type. A separation of the two effects on the basis of bulk data alone is usually very difficult if not impossible.

One of the consequences of intermolecular interactions in solid-state materials is the possibility of energy transfer (ET) upon electronic excitation.[5] The probability of the transfer processes is directly related to the off-diagonal matrix elements of the interaction operator. ET phenomena have been extensively studied in both organic and inorganic materials.[6] For the case of exchange interactions as the dominant ET mechanism, the theoretical basis was laid by Dexter.[5]

Since in CRAC the consequences of electronic excitation can be studied spectroscopically, it may be a good example from which to obtain an estimate of the order of magnitude of intercluster exchange and thus to assess the model proposed by Brown et al. The presence of two inequivalent sets of clusters in the LT phase of CRAC, which complicates the analysis of bulk data, can be advantageously used in the spectroscopy.

Some knowledge of the structural properties of the LT phase of CRAC is important for the discussion of magnetic and spectroscopic properties. We therefore decided to investigate the structural changes occurring with the phase transition by LT X-ray diffraction. The results are presented in section 3. Results of time-resolved luminescence experiments are given in section 4. Estimates of excitation transfer matrix elements and intermolecular exchange parameters are developed in section 5.

## 2. Experimental Section

The preparation of the compound has been described before.[7]

**2.1. X-ray Diffraction.** For the identification of the LT phase, a crystal was grown by slowly cooling an aqueous solution saturated at 75 °C. The crystal was sealed in a capillary immediately after separation, mounted on a Weissenberg camera, and cooled to 190 K by a stream of cold nitrogen gas. The unit cell of the LT phase was determined on an automatic Syntex-$P2_1$ diffractometer equiped with a corresponding LT accessory.

**2.2. Luminescence Spectroscopy.** For all the measurements the luminescence was dispersed by a Spex 1402 double monochromator and detected with a cooled RCA 31034 PM tube. Photon counting was used for the experiments with continuous excitation. A cavity dumped 4-W argon ion laser (Spectra Physics Model 166) was used in conjunction with a Boxcar Averager (PAR 162) to measure luminescence decay curves and time-resolved spectra.

The samples were cooled by a helium gas flow technique.

## 3. Structural Data

Weissenberg photographs of the LT phase of CRAC revealed a number of very weak "new" reflections, not present in the HT phase. The new reflections can be indexed in terms of a unit cell with $c$ twice as large as in the HT phase and $a$, $b$ unchanged. This doubling of the HT unit cell along the $c$ axis leads to a superstructure with the two halves of the LT unit cell no longer crystallographically equivalent. The space group $P2_12_12_1$ for the LT phase follows from the observed extinctions. Space group and unit cell information for both phases is listed in Table I.

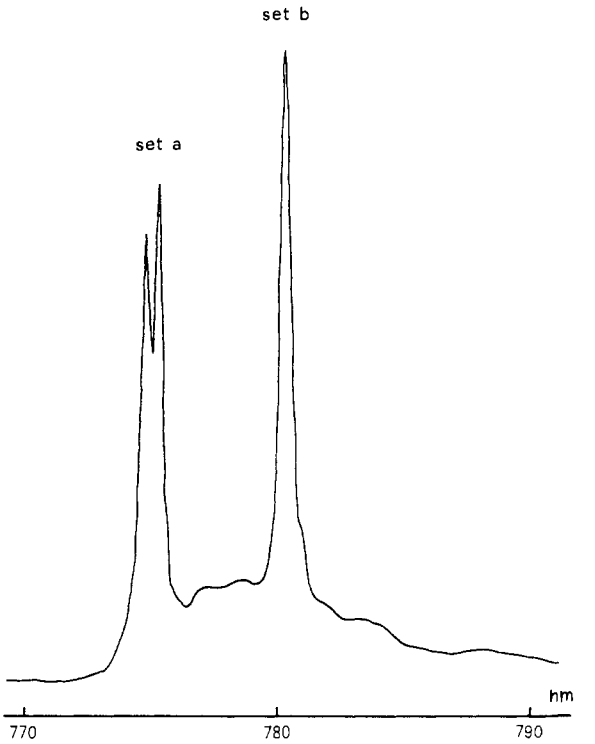


**Figure 1.** Unpolarized 7 K luminescence spectrum of CRAC. Excitation = 514 nm.

In the phase transition the $c$ axis is transformed from a twofold rotation axis (HT) to a twofold screw axis (LT). Molecules which are crystallographically related by the twofold rotation axis around $c$ in the HT phase are no longer equivalent in the LT phase. The eight $Cr_3$ clusters in the LT cell are thus divided into two sets, each set occupying a fourfold general position. A given cluster has five first-nearest-neighbor (1nn) clusters with closest Cr–Cr distances ranging from 5.78 to 6.85 Å. Cr–Cr distances in a next shell of neighbors range from 9.64 Å upward. Intercluster exchange is most likely to be important between 1nn clusters. It is therefore interesting to investigate which of the two inequivalent sets the 1nn clusters belong to. There are two possibilities in space group $P2_12_12_1$: (1) of the five 1nn clusters, two belong to the same set and three to the other; (2) all the 1nn clusters belong to the other set. A full crystal structure determination would be necessary to distinguish between the two possible arrangements. Important for our discussion in the following sections is the fact that interactions between a, b clusters are at least as likely as those between a, a and b, b clusters.

## 4. Spectroscopy

Figure 1 shows the LT luminescence spectrum of CRAC in the region of electronic origins. Vibronic side bands account for only 10–20% of the total luminescence intensity. The two prominent bands near 775 and 780 nm coincide with the corresponding transitions in the absorption spectrum.[4] They are thus identified as intrinsic, whereas part of the background between the two peaks is due to impurities. The 775- and 780-nm emission bands belong to sets a and b, respectively, of clusters. They have different excitation spectra at 7 K.[4]

As shown in Figure 2, the intensities and decay times of both emissions are of comparable magnitude at 7 K. This is in agreement with the crystallographic result that sets a and b of clusters are present in equal proportions. Drastic differences between the two emission bands are observed when the temperature is raised above 20 K: an increase of both intensity and decay time for the low-energy emission up to 35 K, accompanied by a strong decrease for the high-energy emission in the same temperature interval. Intensity and decay time

(5) Dexter, D. L. *J. Chem. Phys.* **1953**, *21*, 836.
(6) Powell, R. C.; Blasse, G. *Struct. Bonding (Berlin)* **1980**, *42*, 43.
(7) Weinland, R.; Dinkelacker, P. *Ber. Dtsch. Chem. Ges.* **1909**, *42*, 2997.

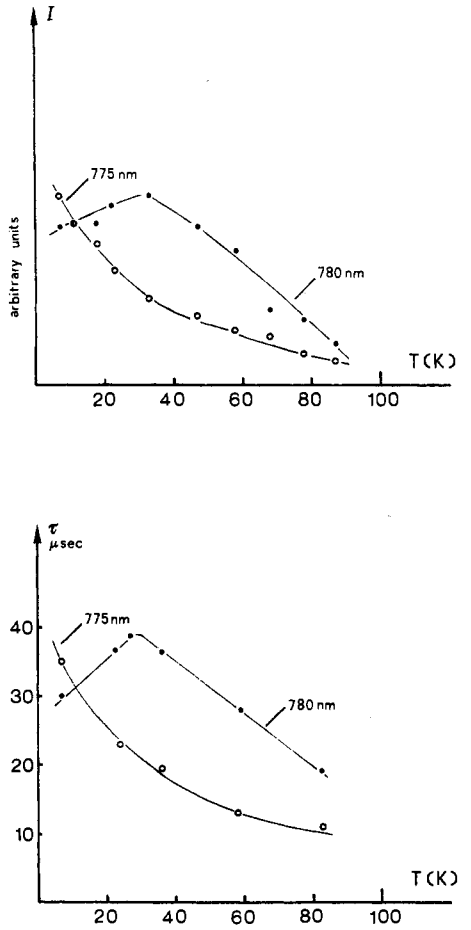


**Figure 2.** Temperature dependence of the intensities and decay times of the two dominant emission bands near 775 and 780 nm. The drawn curves represent a guide for the eye. At higher temperatures the 780-nm emission decays nonexponentially (cf. Figure 5). Decay times were determined between 40 and 80 μs, where the curves are nearly exponential.

of the low-energy emission start to slowly decrease above 35 K but remain significantly higher than the corresponding values for the high-energy emission throughout the investigated temperature range. Two interplaying physical effects are discernible from this temperature dependence: (1) A nonradiative deactivation mechanism is responsible for the overall decrease of intensities and decay times with increasing temperature. (2) Excitation-energy transfer from set a to set b of clusters is responsible for the differences in the behavior of the two emissions. This mechanism is strongly temperature dependent, being inactive at 7 K but competitive with mechanism 1 at temperatures above 20 K.

The ET process can be nicely followed by time-resolved spectroscopy. In Figure 3 emission spectra are plotted for different delay times after the exciting laser pulse. At 30 and 63 K the intensity ratio of high (set a) and low-energy (set b) emission bands decreases with increasing delay. Part of the excitation of set a is being transferred into set b, leading to the observed great disparity of intensities 50 μs after the pulse. The underlying broad impurity emission is very short-lived.

Another piece of evidence for energy transfer at higher temperatures is the shape of the luminescence decay curves. At 7 K they are approximately exponential for both bands. With increasing temperature the 775-nm emission remains exponential, whereas the 780-nm decay curve shows drastic deviations. This is illustrated in Figure 4. Two main effects contribute to the observed shape of the 780-nm emission: (1) exponential decay due to direct excitation of the set b of

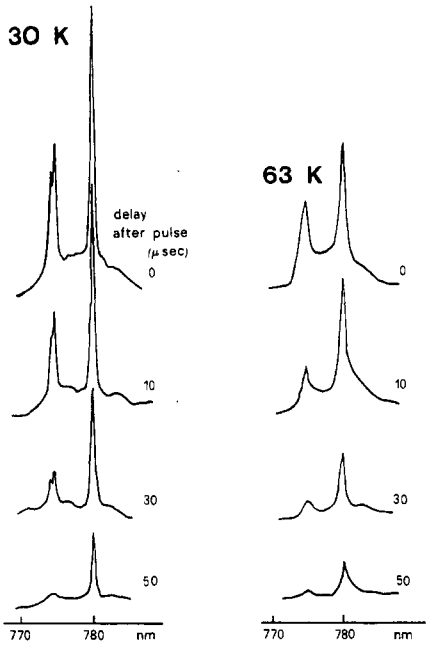


**Figure 3.** Time-resolved emission spectra. Excication pulse width = 5 μs (514 nm).

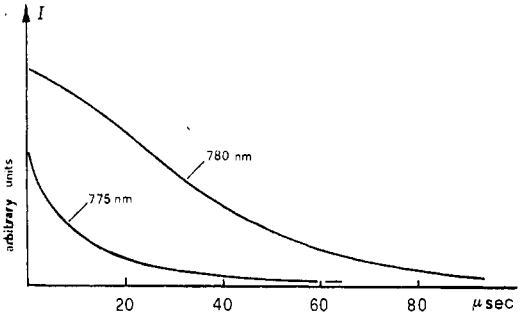


**Figure 4.** Decay curves of 775 and 780 nm emissions at 60 K. Excitation pulse width = 5 μs (514 nm).

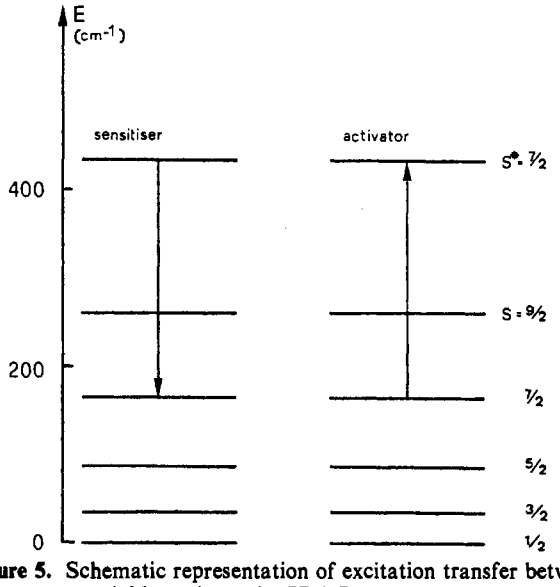


**Figure 5.** Schematic representation of excitation transfer between first-nearest-neighbor trimers in CRAC.

clusters by the pulse; (2) ET from set a of clusters with a rise time corresponding approximately to the decay time of the 775-nm emission. From the data in Figures 3–5 it is clear that ET from set a to b contributes to the nonradiative deactivation of the 775-nm emission at temperatures above 20 K. Since this mechanism is in competition with another nonradiative

Table II. Boltzman Populations of $S = {}^7/_2$ Ground Level

| $T$, K | pop. | $T$, K | pop. |
|---|---|---|---|
| 7 | $2 \times 10^{-10}$ | 58 | $5.1 \times 10^{-2}$ |
| 10 | $2 \times 10^{-7}$ | 63 | $6.0 \times 10^{-2}$ |
| 23 | $1.5 \times 10^{-3}$ | 83 | $9.4 \times 10^{-2}$ |
| 36 | $1.3 \times 10^{-2}$ | | |

mechanism, we can obtain an upper limit for the energy-transfer rate from the 775-nm decay times. From the 83 K data we get: $k_{ET} \leq 1/\tau = 9 \times 10^4$ s$^{-1}$.

## 5. Energy Transfer and Intermolecular Exchange

The electronic ground state of a chromium(III) trimer with regular triangular geometry is split by exchange interactions into five components with total spin quantum numbers $S = {}^1/_2, {}^3/_2, {}^5/_2, {}^7/_2$, and ${}^9/_2$. The splitting is schematically shown in Figure 5. The transition observed in the emission spectrum is from the lowest trimer excited level with $S^* = {}^7/_2$ to the $S = {}^7/_2$ ground level.[4] Transitions with $\Delta S \neq 0$ are less intense by at least 2 orders of magnitude.[4] From absorption spectra the oscillator strength of the $S = {}^7/_2 \rightarrow S^* = {}^7/_2$ transition is estimated to be $f = 2 \times 10^{-7}$/mol of Cr. The corresponding radiative lifetime of the $S^* = {}^7/_2$ excited state is 2 orders of magnitude longer than the measured emission decay times at 7 K. Nonradiative decay mechanisms must therefore be dominant down to the lowest temperatures. The most likely deactivation mechanism at 7 K is a multiphonon process,[8,9] with the molecular high-energy C–H and O–H vibrations as the active modes. This mechanism also plays an important part at higher temperatures. For the high-energy 775-nm emission, competition arises from an ET mechanism above 20 K.

The ET situation between nearest-neighbor clusters in the lattice is schematically depicted in Figure 5. Resonant transfer of energy[6] from an electronically excited cluster can only occur if at least one of its neighbors is thermally excited to the $S = {}^7/_2$ level. The probability of transfer is thus directly proportional to the $S = {}^7/_2$ Boltzman population and the number of nearest neighbors. From the $S = {}^7/_2$ populations in Table II, it is then clear that ET is highly improbable at 7 K. Between 7 and 20 K the probability increases by more than 5 orders of magnitude. It is interesting to draw an analogy between this situation and that of an inert lattice doped simultaneously with sensitizer and activator ions.[6] By changing the temperature we can vary the activator concentration within many orders of magnitude. This provides a convenient way of measuring the concentration dependence of the ET processes.

Transfer between nearest-neighbor clusters belonging to the same crystallographic set is strictly resonant, whereas transfer from set a to set b clusters is slightly off-resonant due to the energy mismatch between the ${}^7/_2 \rightleftarrows {}^7/_2$ transitions. The spectral overlap between the emission of set a and the absorption of set b is not zero, however, due to some finite intensity in the vibronic side bands. From a comparison of absorption and emission profiles the overalp $\Omega$ is estimated to 5%. Back-transfer from set b to set a of clusters is possible at higher temperatures. This is not a dominant contribution, however, and will be neglected in the following considerations.

There is no direct spectroscopic evidence for the ET between clusters of the same set. On the other hand plenty of evidence has been produced in the last section for a → b ET. An upper-limit estimate of the transfer rate at 83 K is $9 \times 10^4$ s$^{-1}$. This ET rate can now be used for an estimate of the order of magnitude of intercluster exchange interactions.

There are a number of possible mechanisms of excitation-energy transfer in molecular solids.[5] The most likely in our situation of very weak electronic transitions is an exchange mechanism. According to Dexter the transfer probability between a sensitizer (S) and activator (A) molecule can be expressed as eq 1,[5] where $g_S(E)$ and $G_A(E)$ are normalized

$$P_{S \rightarrow A} = (2\pi/\hbar)|H_{SA}|^2 \int [g_S(E)][G_A(E)]\, dE \qquad (1)$$

emission and absorption, respectively, band shape functions, and $\int [g_S(E)][G_A(E)]\, dE = \Omega$ is the spectral overlap integral. $H_{SA}$ is an *excitation-transfer matrix element* of the form given in eq 2. For a numerical estimate of $|H_{SA}|$ in CRAC, we have

$$H_{SA} = \langle SA^*|H_{ex}|S^*A\rangle \qquad (2)$$

to take account of the number of nearest neighbors in the lattice and the $S = {}^7/_2$ Boltzman population. Using the 83 K experimental data and eq 1 we obtain $|H_{SA}| \leq 2 \times 10^{-3}$ cm$^{-1}$.

Excitation-transfer matrix elements (eq 2) are usually not directly accessible by experiment. In a number of chromium(III) dimers, numerical values for the off-diagonal matrix elements involving the first singly excited state have been derived from optical spectroscopic data.[10-12] They were found to be of the same order of magnitude or larger than the ground-state exchange parameter $|J|$, so that we can make the approximation $|H_{SA}| \gtrsim |J|$.

We are interested in an order of magnitude estimate of $|J_{ab}|$ and, by analogy, of $|J_{aa}|$ and $|J_{bb}|$, the intercluster exchange parameters between nearest neighbors in CRAC. In the most generous interpretation of our numerical result, we conclude that these parameters must be smaller than 0.1 cm$^{-1}$. If the 1nn of a cluster of a given set all belong to the other set, which corresponds to one of the two possible structural arrangements compatible with the results in section 3, $|J_{aa}|$ and $|J_{bb}|$ must be much smaller than $|J_{ab}|$.

## 6. Conclusions

On the basis of the structural evidence presented in section 3, we are forced to revise some of the assumptions and conclusions of Brown and co-workers. The clusters are equally distributed among sets a and b and not in a proportion of 80/20 as suggested in ref 1. If intermolecular exchange is an effect to be considered for the interpretation of LT heat capacity data, interactions between molecules of different sets are of paramount importance. They were neglected in ref 1. The values of $|J_{aa}|$ and $|J_{bb}|$ must be similar since the relative dispositions of neighboring molecules are very similar for the two sets. According to ref 1 $|J_{aa}|$ is 4 times as large as $|J_{bb}|$.

The upper limit for intercluster exchange parameters in CRAC, as estimated from the energy-transfer properties, is 1–2 orders of magnitude smaller than the values suggested in ref 1. The model by Sorai and co-workers is thus firmly supported by our structural and spectroscopic results. The heat capacity and magnetic susceptibility anomalies below 20 K result from geometrical distortions of the clusters in the LT phase, with set a suffering a bigger distortion than set b.

**Acknowledgment.** We are indebted to G. Chapuis and D. Schwarzenbach for valuable suggestions in the course of the X-ray work and the use of their instrumentation. This work was financially supported by the Swiss National Science Foundation (Grant No. 2.427-079).

**Registry No.** $[Cr_3O(CH_3COO)_6(H_2O)_3]Cl \cdot 6H_2O$, 32591-52-9.

(8) Strek, W.; Ballhausen, C. J. *Mol. Phys.* **1978**, *36*, 1321.
(9) Englman, R. "Non-radiative Decay of Ions and Molecules in Solids"; North-Holland Publishing Co.: Amsterdam, 1979; p 78.
(10) Dubicki, L. *Aust. J. Chem.* **1972**, *25*, 739.
(11) van Gorkom, G. G. P.; Henning, J. C. M., van Stapele, R. P. *Phys. Rev. B: Solid State* **1973**, *8*, 955.
(12) Dubicki, L.; Ferguson, J.; Harrowfield, B. V. *Mol. Phys.* **1977**, *34*, 1545.